Stark Spectroscopy of Size-Selected Helical H-Aggregates of a Cyanine Dye Templated by Duplex DNA. Effect of Exciton Coupling on Electronic Polarizabilities[†]

Arindam Chowdhury, Liping Yu, Izzat Raheem,[‡] Linda Peteanu,*,[§] L. Angela Liu, and David J. Yaron*,[‖]

Department of Chemistry, Carnegie Mellon University, Pittsburgh, Pennsylvania 15213

Received: August 12, 2002; In Final Form: February 24, 2003

Stark spectroscopy (electroabsorption) is used to study the variation of electronic properties with the size of helical H-aggregates that are formed by the spontaneous noncovalent assembly of co-facial dimers of the cyanine dye ($DiSC_2(5)$) into the minor groove of double-helical DNA. The unique and important property of these aggregates, first synthesized and characterized by Armitage and co-workers (*J. Am. Chem. Soc.* **1999,** *121,* 2987), is that their size is controlled by the properties of the DNA template. Specifically, the length of the aggregate formed is determined by the length of the DNA template and its width along the π stacking dimension is restricted to that of the dye dimer due to steric constraints in the minor groove. Results for aggregates consisting of 1, 2, 5, and ∼35 adjacent dimers bound to DNA are presented here. The absorption maxima of these species exhibit a large blue shift (1750 cm^{-1}) from that of the monomer due to the face-to-face interactions within the dimers. Relatively weak (330−650 cm^{-1}) secondary splittings are also seen that arise from end-to-end interactions between adjacent dimers on the chain. The average change in polarizability on excitation ($\langle\Delta\alpha\rangle$) is found to double when two dyes form a stacked dimer whereas no further increase in $\langle\Delta\alpha\rangle$ is seen as the chain length is increased. Semiempirical (INDO−SCI) calculations yield exciton coupling energies that are consistent with experiment. However, $\langle\Delta\alpha\rangle$ is predicted to increase toward more positive values on dimerization while the reverse trend is seen experimentally. Nonetheless, both experiment and theory find that $\langle\Delta\alpha\rangle$ is unaffected by higher aggregation.

Introduction

Molecular aggregates that result from the noncovalent association of similar molecules in solution or in a nematic state are important in chemistry, biology,[1] and materials science.[2] For example, aggregates formed from organic and polymeric chromophores that absorb and emit light in the visible region have wide applications as photographic sensitizers,[3] and liquid crystalline displays.[4] They have also been used as nonlinear optical materials due to their large hyperpolarizabilities.[5] Nature uses the electronic properties of such aggregates in light-harvesting systems where arrays of chlorophyll chromophores are responsible for the energy transfer in photosynthetic reaction centers.[6]

Jelly[7] and Scheibe[8] were the first to identify highly fluorescent J-aggregates that show a characteristic red shift in their absorption maxima compared to that of the monomer species. H-aggregates on the other hand, are nonfluorescent and show a characteristic blue shift in their absorption spectrum relative to the monomer.[9,10] To explain the distinct absorption and fluorescence properties of the H- and the J-aggregates, Kasha et al.[11−15] developed a theoretical treatment for molecular aggregates based on the exciton-coupling model of molecular crystals.[16] Exciton-coupling theory predicts that noncovalent dimerization (or polymerization) of dyes within an aggregate lowers the degeneracy of its excited electronic state compared to the uncoupled monomers. For H-aggregates, the higher electronic state carries all of the oscillator strength while transitions to the lower electronic (exciton) state are forbidden. As a result, the absorption of the aggregate is blue-shifted and its fluorescence is effectively quenched because internal conversion to the lowest (forbidden) excitonic state is faster than emission, in accordance with Kasha's rules. In contrast, for J-aggregates, the transition to the lowest exciton state is allowed. This, in turn, gives rise to a red shift and narrowing of the absorption spectrum relative to that of the monomer and a strong fluorescence emission having a negligible Stokes shift.

The consequence of this coupling on the electronic properties of the aggregate is strongly dependent on the relative orientation of the transition moments of the constituent molecules and therefore on the stacking pattern that they adopt.[17] To produce a blue-shifted absorption maximum, as for H-aggregates, the arrangement of the stacked dyes must be such that the slippage angle, α, formed between the (parallel) transition dipoles and the line joining the centers of the dipoles, is greater than 54.7°.[13,15,18] In contrast, to produce the red shift observed for J-aggregates, the stacked chromophores must be laterally shifted with respect to one another such that this angle is less than 54.7°.[13,15,18] In the literature, H-aggregates are often referred to as having a card-pack structure, while J-aggregates are said to resemble a brickwork arrangement. For more details see refs 13 and 15.

Control over the structure and the number of molecules constituting a noncovalent molecular aggregate is crucial to controlling its resulting electronic and optical properties. This is in turn important to optimizing these materials for applications such as those cited above.[19] In practice, for noncovalent
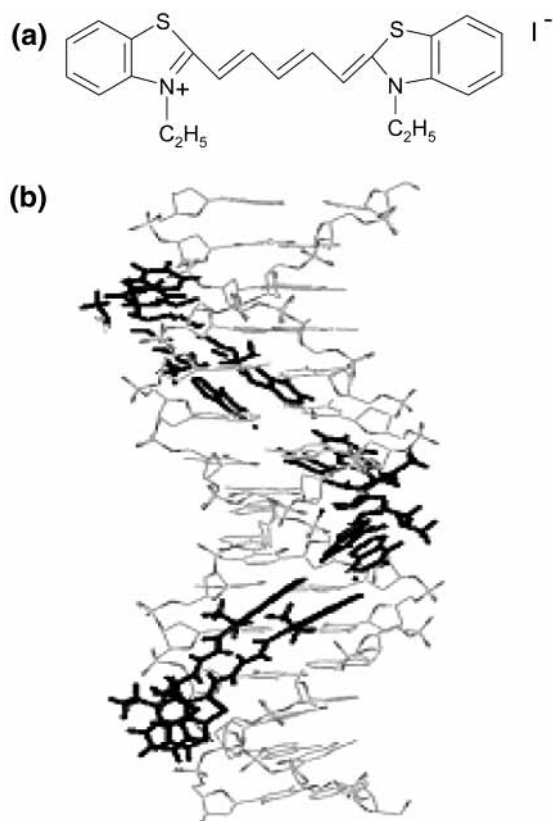
Figure 1. (a) 3,3′-Diethylthiadicarbocyanine iodide (DiSC$_2$(5)). (b) Model of three adjacent H-dimers of DiSC$_2$(5) bound to double-helical DNA.

aggregates formed freely in solution, such control is difficult to achieve due to their high degree of sensitivity to environmental conditions such as the temperature, polarity, ionic strength, and pH of the solution.[19−23]

Recently Armitage et al. have shown that a particular class of cyanine dyes known as DiSC$_2$(5) (3,3′-diethylthiadicarbocyanine iodide, Figure 1a), noncovalently assembles into the minor groove of double-helical DNA such that *two* DiSC$_2$(5) molecules form a face-to-face dimer.[24] Stacking of additional dyes is prevented due to the constraint imposed by the walls of the minor groove. However, because binding of one such dimer is thought to widen the minor groove, the assembly of additional dimers on the adjacent sites is more favorable. In this fashion, an extended aggregate can be formed. These species display the blue-shifted absorption spectrum and reduced fluorescence yield that is characteristic of H-dimers and higher aggregates. When assembled in the minor groove of DNA, the dye dimers are forced to acquire a helical structure. This model is strongly supported by electronic absorption and circular dichroism (CD) spectroscopies.[24−26] Figure 1b shows a model of dye dimers bound to a double-stranded DNA, as proposed by Armitage and co-workers.[24]

Another desirable feature of using DNA templates is that the number of dye molecules present in a given aggregate can be controlled by the length and the sequence of the DNA chosen. Because the presence of guanine bases sterically hinders the assembly of dyes into the minor groove, introduction of guanine into the sequence effectively disrupts the growth of the aggregate.[24,25] Replacing guanine bases with the artificial nucleobase inosine allows the dyes to spontaneously assemble onto the DNA. Since a single cofacial H-dimer of DiSC$_2$(5) spans about half a turn of the helix (approximately five base pairs), the length of the aggregate can be controlled by changing

the length of the inosine containing region of the DNA template in increments of five base pairs.

The scaling of important optical properties of aggregates, such as the extinction coefficient,[14] fluorescence quantum yield,[27−30] radiative lifetime,[18,31] and line width of absorption and emission,[32,33] with respect to the corresponding properties of the monomer, depends critically on the *spectroscopic aggregation number*, which we designate here as N_C. N_C is the number of chromophores in the aggregate that are coherently coupled, or collectively excited upon absorption of a photon.[34] N_C is expected to be smaller than the actual number of molecules constituting the molecular aggregate due, most likely, to disorder.[18,35] Collective (coherent) excitation of N_C adjacent dipoles leads to a N_C-fold increase of the probability of absorption[14,18] and emission,[27,28] which in turn enhances non-linear properties such as the first hyperpolarizability of dye aggregates.[5]

Because N_C directly correlates to the important linear and nonlinear optical properties of aggregates, there has been considerable effort to determine how its value is affected by aggregate size, structure, composition, and the presence or absence of defects. Radiative lifetime measurements on fluorescent J-aggregates of pseudoisocyanine (PIC) performed over a range of temperatures (4−130 K) have estimated N_C to be between 10 and 50,[23] while hole burning measurements suggested a value of 100 for the N_C of aggregates of the same dye.[36] Using a photon-echo technique, Wiersma measured a value of N_C of ~500 for PIC J-aggregates in a glassy matrix.[37] Kobayashi et al. performed linear dichroism and Stark spectroscopic studies on PIC J-aggregate films. They compared the change in the electronic polarizability on excitation ($\langle \Delta \alpha \rangle$) of the monomer to that of the aggregates and inferred that $\overline{N_C}$ ranges from 20 to 100.[38,39] Note that many of these methods rely on fluorescence and therefore are *only* suitable for measuring the properties of J-aggregates.

Important for the current study is that it has been proposed that the ratio of the $\langle \Delta \alpha \rangle$ of the aggregate to that of the monomer will scale with $\overline{N_C}$ since N_C is effectively a measure of the extent of delocalization of the excited state.[38,40,41] This ratio, *which we refer to as the enhancement factor for* $\langle \Delta \alpha \rangle$, can be measured using Stark spectroscopy, a technique that is equally applicable to J- and H-type aggregates.

The work described here follows up on an earlier publication in which we examined the scaling of $\langle \Delta \alpha \rangle$ with aggregate type (H vs J) in aggregates that were *not* size-selected. There, $\langle \Delta \alpha \rangle$ for the J-aggregate was reported to be five to six times that of the monomer while $\langle \Delta \alpha \rangle$ for the H-aggregate was found to be only twice the monomer value. These results were rationalized in terms of the different structures of these two species. Specifically, the card-pack structure of the H-aggregates is expected to afford strong coupling within a given dimer but weak couplings between adjacent dimers. In contrast, the brickwork J-aggregate structure should allow stronger interactions between dyes adjacent to one another along the aggregate chain.

To assess whether the enhancement factor for $\langle \Delta \alpha \rangle$ provides an alternative method of characterizing N_C for aggregates, as was originally suggested in ref 38, we compared its value for the J-aggregates to that of N_C obtained by the well-established methods of fluorescence lifetime[28,31] and line-width measurements.[32,33] Indeed, the value of N_C obtained via these methods agreed with the enhancement factor of $\langle \Delta \alpha \rangle$ for the J-aggregate to within a factor of 2. This level of agreement is

Stark Spectroscopy of Helical H-Aggregates

J. Phys. Chem. A, Vol. 107, No. 18, 2003 **3353**

certainly reasonable given the spread of values typically found in the literature for N_C, several examples of which are quoted above. On the basis of this comparison, it appeared that measurements of the enhancement factor for $\langle\Delta\alpha\rangle$ might indeed provide an alternative means of characterizing N_C for J-type and, by extension, for H-type aggregates. Unfortunately, analogous comparisons for H-aggregates are not possible using fluorescence-based methods.

The current study exploits the fact that H-aggregates of precisely defined size can be formed via DNA templating. Therefore, in principle, N_C can be compared to the actual physical size of the aggregate, which has *not* been possible in prior studies in the literature. Similar experiments could not be performed for J-aggregates because, even when DNA is used as a scaffold, they do not assemble as small size-selected aggregates. This is probably due to the highly cooperative interactions needed to stabilize the brickwork structure.

This paper summarizes a joint experimental and computational study with the aim of understanding how the electronic properties of aggregates vary with aggregate size and structure. First, the absorption and electroabsorption spectra of a series of H-aggregates consisting of a single dimer, as well as two, five, and ∼35 adjacent dimers are presented. From the absorption spectrum of each aggregate, the exciton splittings due to end-to-end interactions of adjacent dimers are obtained. The saturation value of this splitting vs aggregate size, which we argue is a direct measure of N_C for these species, occurs for aggregates consisting of more than six dimers. For comparison, the enhancement factor for $\langle\Delta\alpha\rangle$ for each aggregate is reported. This quantity is found to be 2 for all of the aggregates, regardless of size. Therefore, unlike what had been suggested earlier for J-aggregates, the enhancement factor of $\langle\Delta\alpha\rangle$ appears to be a poor indicator of the value of N_C in H-aggregates.

Following the experimental studies, semiempirical quantum chemical calculations are presented that model the effects of aggregation on the absorption spectrum and on the value of $\langle\Delta\alpha\rangle$. Modeling of the exciton shifts and splittings indicates that both are consistent with the expected structure of the H-aggregates on the DNA template. Theory also agrees with the experimental finding that the calculated $\langle\Delta\alpha\rangle$ changes substantially between monomer and a single H-dimer but is unaffected by coupling between two adjacent H-dimers. However, two fundamental and as yet unresolved discrepancies between theory and experiment emerge. The first regards the sign of $\langle\Delta\alpha\rangle$ of the monomer, which is negative experimentally but is calculated to be positive for most reasonable geometric parameters for the dye. The second is the direction of the calculated change in $\langle\Delta\alpha\rangle$ upon formation of a single dimer from two stacked monomers. Experiment finds $\langle\Delta\alpha\rangle$ of the dimer to be more negative than that of the monomer whereas theory finds the opposite. Several efforts to determine the origin of these discrepancies are presented but are as yet inconclusive.

The paper concludes with a summary of the results that have been obtained for both J- and H-type aggregates and relates these to the different stacking geometries expected in these two systems.

Experimental Section

Materials and Methods. 98% pure $DiSC_2(5)$ (3,3′-diethylthiadicarbocyanine iodide) was obtained from Aldrich Chemicals and used without further purification. All of the synthetic DNAs were obtained from Integrated DNA Technologies (IDT). The desired $DiSC_2(5)$ H-dimers and H-aggregates are readily obtained by mixing the solutions of duplex DNA, in sodium phosphate buffer, pH 7.2, and the dye in appropriate molar ratio. Room-temperature absorption spectra were obtained after allowing the solution to mix for 10 min. The disappearance of the monomer peak at 655 nm and the appearance of a new band at ∼590 nm indicate that the assembly of the dye into the DNA in dimer form is essentially quantitative. The shifts in the absorption maxima observed are in agreement with that first found by Armitage and co-workers[24] and are correlated with the formation of H-dimers/aggregates in the DNA minor groove. All experiments were performed in 35% ethylene glycol−water (EG−water) glass at 77 K. The pH was maintained at 7.2 using a 10 mM phosphate buffer.

It was empirically found that slowly lowering the temperature of the solution minimizes the number of monomeric dyes present in the sample cell. This is because the binding constant of the dye to the DNA increases as the temperature is lowered.[24,25] Therefore, to optimize aggregate formation, the temperature of the sample cell was first held at ∼200 K for 2 min by suspending it just *above* the liquid nitrogen surface. Then, to obtain the Stark spectrum at 77 K, the cell was fully immersed into liquid nitrogen to form an optically clear glass.

To obtain the 77 K spectra of the monomeric dyes and to minimize the formation of random aggregates in solution, $DiSC_2(5)$ was dissolved in a 80% ethylene glycol and 20% methanol solution and the sample cell was immersed into liquid nitrogen. The dye concentration was maintained so as to have a sample absorbance of between 0.1 and 0.8, with the DNA concentration adjusted accordingly.

A sample of monomeric $DiSC_2(5)$ *bound to the DNA minor groove* was formed using an excess of poly(dA)−poly(dT) duplex, such that the $DiSC_2(5)$ dye would preferentially bind in the monomeric form. While it would be desirable to use 1 dye for every 15−20 DNA base pairs, at such low dye concentrations, the absorbance of the sample was too low (<0.02) and the Stark signal was below our detection limits. To obtain a measurable absorbance (∼0.03) and Stark signal, the $DiSC_2(5)$ concentration was maintained such that there was a single $DiSC_2(5)$ molecule for every six to eight base pairs of the DNA.

Synthetic duplex DNAs of varying lengths were used as templates. Since guanine has an amino group that protrudes into the minor groove and sterically hinders the binding of dyes, guanine−cytosine base pairs were chosen as terminal bases as well as spacers between dye dimers so as to vary the distance between them. An artificial base inosine (guanine without an amino group) was used in the templating regions. H-dimers/aggregates are readily formed in the presence of the inosine−cytosine base pairs.[42] Each H-dimer spans about half a turn of the DNA helix which translates to approximately five base pairs for every H-dimer.[24] A single isolated H-type dimer of $DiSC_2$-(5) was formed using the following double-stranded **(IC)₅** DNA template.

5′-CGC-**ICICI**-CGC-3′

3′-GCG-**CICIC**-GCG-5′

The ratio of the duplex **(IC)₅** DNA to $DiSC_2(5)$ was maintained at 1:2. Two noninteracting H-dimers of $DiSC_2(5)$, separated by three guanine−cytosine base pairs, were formed using the **²(IC)₅** DNA duplex shown below:

5′-CGC-**ICICI**-GCG-**ICICI**-CGC-3′

3′-GCG-**CICIC**-CGC-**CICIC**-GCG-5′
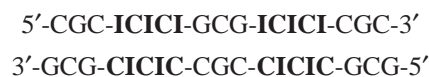
(IC)₁₀ (10 inosine−cytosine base pairs) and **(IC)₂₅** (25 inosine−cytosine base pairs) sequences were used to form *two* and *five* adjacent H-dimers, respectively. The **(IC)₂₅** DNA template purchased was purified by PAGE electrophoresis in order to remove smaller DNA fragments. This proved critical for obtaining well-resolved absorption spectra of these aggregates. Double-stranded poly(dI−dC) containing 150−160 inosine−cytosine base pairs was used to form multiple adjacent H-dimers of DiSC₂(5). It was inferred that ∼35 ± 5 H-dimers comprise this aggregate because the addition of more dyes resulted in the appearance of an absorption band in the monomer region (∼655 nm). Roughly 20 guanine−cytosine base pairs were used as terminal bases on both 3′- and 5′-ends of each DNA.

Electroabsorption Data Analysis. The electroabsorption apparatus is home-built and has been previously described in detail.[43−45] The analysis of the electroabsorption data follows that in the literature.[46,47] The equations shown here are appropriate for the experimental conditions used; i.e., the sample is isotropically embedded in a rigid glass. Essentially, the change in absorption due to the application of an external electric field is fit to the weighted sum of zeroth, first, and second derivatives of the zero-field absorption spectrum. The overall change in absorbance caused by the application of an electric field can be described as follows:

$$\Delta A(\tilde{\nu}) = \vec{\mathbf{F}}_{eff}{}^2 \left[\mathbf{a}_\chi A(\tilde{\nu}) + \mathbf{b}_\chi \frac{\tilde{\nu}}{15\hbar} \left\{ \frac{\partial}{\partial\tilde{\nu}} \left(\frac{A(\tilde{\nu})}{\tilde{\nu}} \right) \right\} + \mathbf{c}_\chi \frac{\tilde{\nu}}{30\hbar^2} \left\{ \frac{\partial^2}{\partial\tilde{\nu}^2} \left(\frac{A(\tilde{\nu})}{\tilde{\nu}} \right) \right\} \right] \tag{1}$$

The term $A(\tilde{\nu})$ represents the unperturbed absorption as a function of frequency ($\tilde{\nu}$) and $\vec{\mathbf{F}}_{eff}$ represents the field at the sample in V/cm. This effective field includes the enhancement of the applied field due to the cavity field of the matrix. The subscript χ represents the angle between the direction of the applied electric field and the electric field vector of the linearly polarized light. All of the experiments reported here were performed $\chi = 54.7°$ (magic angle). At $\chi = 54.7°$, the expressions of $\mathbf{a}_\chi$, $\mathbf{b}_\chi$, and $\mathbf{c}_\chi$ are related to the change in the transition moment polarizability (A_{ij}) and hyperpolarizability (B_{ijj}), the change in the electronic polarizability ($\langle\Delta\alpha\rangle$), and the change in the dipole moments ($|\Delta\mu|$) respectively, as given in eqs 2−4 below.

$$\mathbf{a}_{54.7} = \frac{1}{3|\vec{m}|^2} \sum_{i,j} A_{ij}{}^2 + \frac{2}{3|\vec{m}|^2} \sum_{i,j} m_i B_{ijj} \tag{2}$$

$$\mathbf{b}_{54.7} = \frac{10}{|\vec{m}|^2} \sum_{i,j} m_i A_{ij} \Delta\mu_j + \frac{15}{2} \langle\Delta\alpha\rangle \tag{3}$$

$$\mathbf{c}_{54.7} = 5|\Delta\mu|^2 \tag{4}$$

In this work we quote $\langle\Delta\alpha\rangle$ which represents the average change in electronic polarizability between the ground and excited state (i.e., $\langle\Delta\alpha\rangle = {}^1/_3 \text{Tr}(\langle\Delta\alpha\rangle)$). Information regarding $|\Delta\mu|$ for the molecule is contained in the c₅₄.₇ term (eq 4). It is important to emphasize that, for an isotropic sample such as those studied in this work, only the magnitude and not the sign of $|\Delta\mu|$ is measured. In the above equations, the tensors $\underline{A}$ and $\underline{B}$ represent the transition polarizability and hyperpolarizability, respectively. These describe the effect of $\vec{\mathbf{F}}_{eff}$ on the molecular transition moment: $\vec{m}$ ($\vec{\mathbf{F}}_{eff}$) = $\vec{m}$ + $\underline{A}\cdot\vec{\mathbf{F}}_{eff}$ + $\vec{\mathbf{F}}_{eff}\cdot\underline{B}\cdot\vec{\mathbf{F}}_{eff}$. These terms are generally small for allowed transitions and can therefore be neglected relative to other terms in the
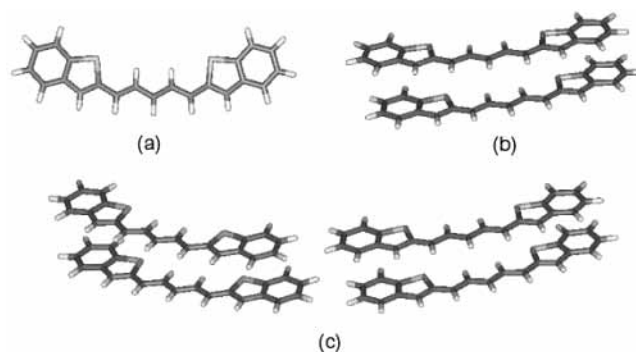

Figure 2. Model structures of (a) the DiSC₂(5) monomer, (b) an isolated H-dimer of DiSC₂(5), and (c) two interacting adjacent H-dimers of DiSC₂(5) that were used for semiempirical (INDO/SCI) calculations.

expression for $\langle\Delta\alpha\rangle$ (eq 3), particularly in those species exhibiting a small value of $|\Delta\mu|$, such as those reported here.

The coefficients, $\mathbf{a}_\chi$, $\mathbf{b}_\chi$, and $\mathbf{c}_\chi$, are extracted by means of a linear least-squares fit of the electroabsorption signal to the sum of the derivatives of $A(\tilde{\nu})$. If the resultant fit to the absorption line shape (a single set of $\mathbf{a}_\chi$, $\mathbf{b}_\chi$, and $\mathbf{c}_\chi$) is not of high quality, this is an indication that there is more than one transition (electronic or vibronic) underlying the absorption band, each having different electrooptical properties. This is *not* found to be the case for the systems studied in this work. Our fitting strategies are described in detail in ref 44.

Semiempirical Calculations. The geometry of a single cyanine dye was optimized at the HF/6-31G** level using the Gaussian software package.[48] The resulting geometry, shown in Figure 2a, is planar. The difference between the single and double bonds of Figure 2a, defined as the bond length alternation (BLA), is less than 0.001 Å. In some of the calculations shown below, this structure is altered to allow control of the BLA and planarity of the system. This is done by dividing the molecule into seven segments, consisting of the two terminal ring structures and the five CH groups of the central polyene. The molecule lies in the $X-Y$ plane with the X-axis connecting the carbon atoms of the rings to which the polyene is attached. The BLA of the polyene was controlled by displacing the segments along the X axis to obtain the desired BLA, while maintaining an average CC bond length of 1.386 Å (the average bond length obtained from the ab initio calculations). The effects of nonplanarity are explored by twisting the segments in a spiral about the X-axis. The twist is reported as the angle between the rings, with the angle between adjacent segments being $^1/_6$th that of the total inter-ring twist.

Dimers were made by stacking the monomers face-to-face with a lateral shift, s, of one of the monomers along the X-axis and an interplane spacing, d, in the Z-direction. Figure 2b shows a dimer with $s = 0$ and $d = 4$ Å. A quadramer structure was made by placing identical dimers along the X-axis, such that the closest contact between terminal hydrogen atoms is ∼2.5 Å (Figure 2c). This procedure was also used for nonplanar monomers, with the XY plane positioned to bisect the twist angle between the two rings.

Finite field calculations described by Kurtz et al.[49] were carried out at the INDO/SCI level, using a direct SCI method[50] that allows for the inclusion of all single excitations. The applied field was 5×10^5 V·cm⁻¹ (9.7×10^{-5} au), and the polarizability was obtained as the first derivative of the calculated dipole moments.

The effects of charge transfer between molecules within an aggregate were investigated using local orbitals and controlling
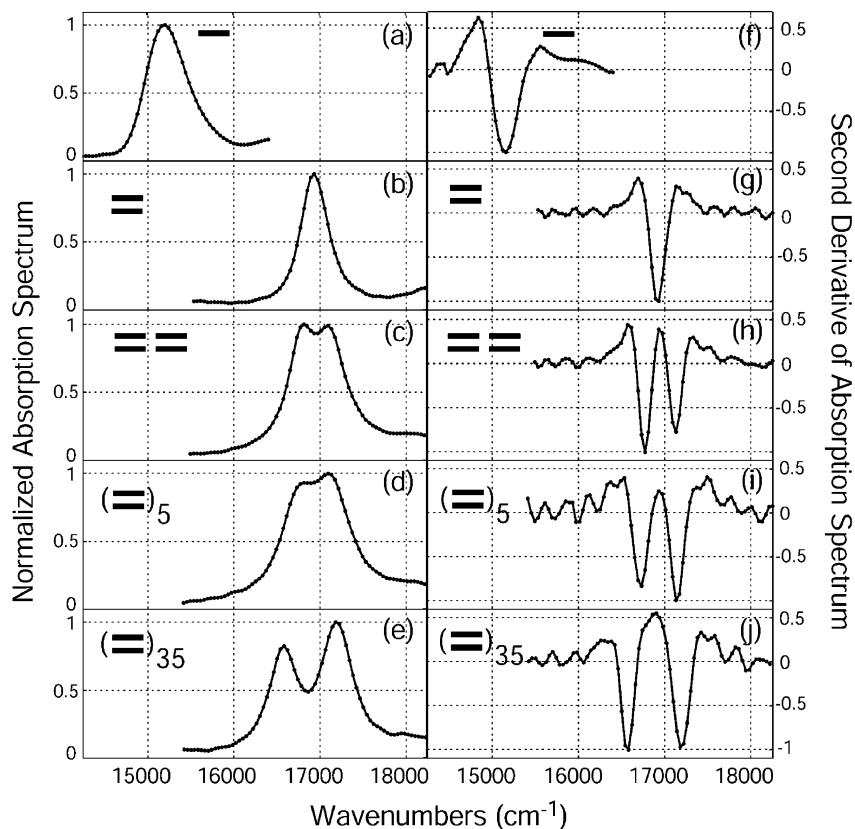
Stark Spectroscopy of Helical H-Aggregates

J. Phys. Chem. A, Vol. 107, No. 18, 2003 **3355**

Figure 3. Normalized 77 K absorption spectra (left panels) and the corresponding second derivative of the normalized absorption spectra (right panels) of, from top to bottom, the monomer DiSC$_2$(5), an isolated H-dimer, two adjacent H-dimers, five adjacent H-dimers, and an H-aggregate of DiSC$_2$(5) having approximately 35 adjacent H-dimers. Each of the heavy bars in the legend represents a dye monomer.

the SCI basis set. Orbitals localized on each of the cyanine dyes were formed using a projection method.[51] A Hartree−Fock calculation is first performed on each of the dye molecules to obtain "target" local orbitals. The delocalized canonical Hartree−Fock molecular orbitals of the aggregate are then used to construct projection operators onto the filled and empty orbital spaces of the aggregate. These projection operators are applied to the target local orbitals and this is followed by Löwdin orthogonalization. This procedure leads to local orbitals that are related to the canonical (delocalized) Hartree−Fock orbitals by a unitary transformation within the filled or empty orbital spaces. The formation of local orbitals therefore has no effect on the results of a SCI calculation that includes excitations between all filled and empty orbitals. However, local orbitals allow us to turn off charge-transfer by constructing a SCI basis that includes excitations only between orbitals that are on the same molecule.

Results and Discussion

77 K Absorption Spectra. The absorption spectra of monomeric DiSC$_2$(5) in EG−water glass and the various H-dimers/aggregates that are formed in the presence of double-stranded DNA are shown in the left column of Figure 3. The monomer (Figure 3a) has an absorption maximum of 15200 cm^{-1} in this matrix. Below, we show that this spectrum is only weakly shifted upon binding of the monomer to DNA.

In the presence of the duplex (IC)$_5$ sequence, a single (isolated) face-to-face (H-Type) dimer is formed, resulting in a ∼1700 cm^{-1} blue shift of the absorption maximum (Figure 3b). The origin of the shift can be understood from the energy diagram shown in Figure 4. This blue shift is a result of the splitting of the excited electronic states in the H-dimer due to
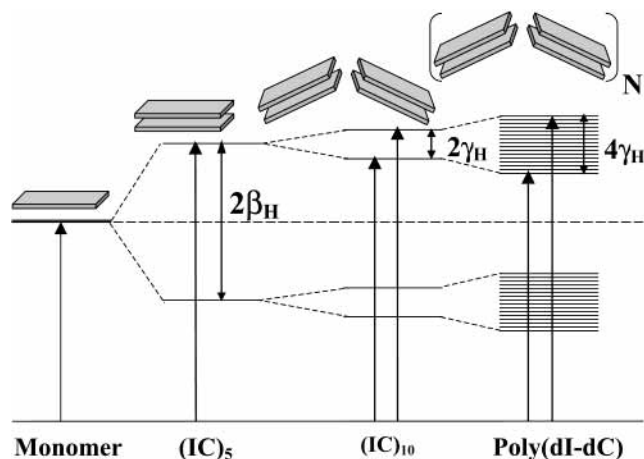

Figure 4. Proposed energy level scheme for various H-aggregates formed by the assembly of DiSC$_2$(5) onto duplex DNA. Cartoon structures of the dye monomer, H-dimer and H-aggregates are shown for illustration purposes. The allowed transitions to the exciton states observed in the absorption spectra are shown by arrows. The primary splitting ($2\beta_H$) results from the stacking interaction between cyanine dimers and the secondary splitting ($2\gamma_H$) arises from head-to-tail interactions between neighboring H-dimers.

a strong face-to-face interaction (exciton coupling) of the two monomeric dyes. It will be referred to as the primary splitting (denoted by $2\beta_H$) and it is twice the value of the primary (exciton) coupling energy β_H.

When longer DNA sequences such as (IC)$_{10}$ or (IC)$_{25}$ duplex are used, the single transition for the single H-dimer, centered at 16930 cm^{-1}, splits into two new transitions (Figure 3c,d), that are highlighted in the second derivatives of the absorption spectrum (Figure 3h,i). For the poly(dI−dC) DNA (Figure 3e),

TABLE 1: Coupling Energies and Relative Oscillator Strengths of H-Aggregates

H-aggregates of DiSC$_2$(5)		coupling energy[a]		relative oscillator strengths[b]	
DNA templates	no. of H-dimers	β_H	γ_H	lower state	upper state
(IC)$_5$	1	1740			
(IC)$_{10}$	2	1750	165	1 (0.02)	1
(IC)$_{25}$	5	1735	210	0.9 (0.02)	1
poly(dI-dC)	35 ± 5	1680	320	0.8 (0.02)	1

[a] From the second derivative spectrum, in cm^{-1}; errors are ± 25 cm^{-1}. [b] From 77 K absorption spectrum.

the absorption maxima of the two transitions shift further apart such that two well-resolved bands are observed. This splitting (Figure 3c−h), which results from the head-to-tail interaction of two (or more) H-dimers lying adjacent to one another, will be referred to as the secondary splitting (denoted by $2\gamma_H$) and is twice the value of the secondary coupling energy (γ_H). For all systems studied, $2\gamma_H$ is much smaller than $2\beta_H$ (Table 1).

Focusing first on the primary coupling energies, β_H is $\sim$1700 ± 50 cm^{-1} for all the H-aggregates studied here though it *decreases* slightly (by 70 cm^{-1}) for the poly(dI−dC) sequence (Table 1) indicating a weaker face-to-face interaction of the two dyes in the individual H-dimers in the extended aggregate. Chowdhury et al. have previously observed that the primary coupling is very sensitive to the extent of the face-to-face overlap between two dyes in the individual dimers.[52] We therefore speculate that, in poly(dI−dC), one of the dyes in the individual H-dimers is slightly shifted with respect to the other, resulting in a small reduction of the value of β_H.

The value of γ_H, evaluated directly from the two minima in the second derivatives (Figure 3h−j and Table 1), increases monotonically when the number of the adjacent dimers is increased from 2 to 35. We also see that increasing the distance of separation (by three guanine−cytosine base pairs) between the adjacent H-dimers by using the ^{2}(IC)$_5$ sequence reduces γ_H so much that the two transitions due to head-to-tail coupling can no longer be observed in the absorption spectrum.

The exciton coupling model predicts that for W-shaped (alternate-translational chain) aggregates,[13,53] the value of the splitting energy for N interacting dimers ($N \gg 1$) is expected to be twice that of two interacting dimers ($N = 2$). This effect, which is observed in the absorption spectra, is a consequence of there being *two* neighboring dimers for *each* H-dimer in the polymeric H-aggregate rather than only *one* adjacent H-dimer when the short DNA sequence ((IC)$_{10}$) is used.[15] That the observed γ_H of the long chain (poly(dI−dC)) is roughly twice that observed for two interacting dimers suggests that the optical excitation is substantially delocalized.

To quantify the degree of delocalization we consider a simple exciton coupling model and calculate the dependence of γ_H on chain length (Figure 5). The model uses a Hückel-like matrix whose dimension is the number of coupled H-dimers. All of the diagonal matrix elements are identical and are equal to the excitation energy of a single H-dimer. The coupling between adjacent H-dimers is taken to be the experimental value of 165 cm^{-1} observed for two adjacent H-dimers. γ_H is the difference in energy between the uppermost and lowermost states obtained from diagonalizing this matrix. Calculated and experimental values are shown in Figure 5. Note that the experimentally observed doubling of γ_H is consistent with a minimum value of the delocalization length of 6−8 dimers. The fact that the value for (IC)$_{25}$ ($N = 5$) is substantially lower than that predicted by the model may indicate a somewhat looser packing of dye
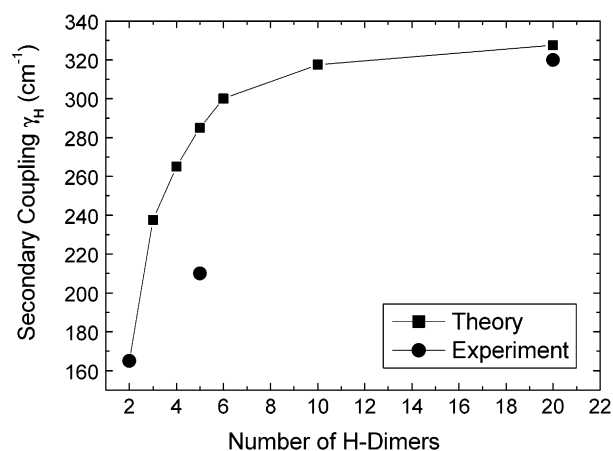

Figure 5. Calculated secondary coupling energies (γ_H, filled squares) obtained via a Hückel-type calculation and scaled with respect to the experimental value of γ_H (165 cm^{-1}) for two adjacent dimers, plotted against the number of H-dimers in the aggregate. The experimental values of γ_H (filled circles) for two, five, and $\sim$35 interacting H-dimers are also shown. The error in the measured value of γ_H is ±25 cm^{-1}.
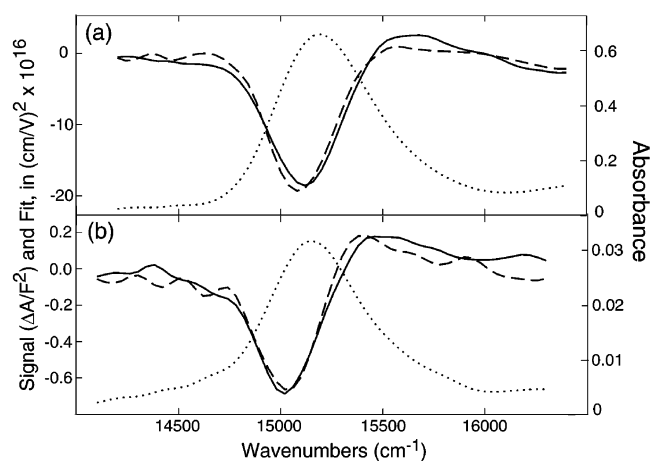

Figure 6. (a) Electroabsorption spectrum (solid line) and fit (dashed line) for the monomer in EG/water glass. (b) Electroabsorption spectrum (solid line) and fit (dashed line) for the monomer bound to DNA in EG/water glass. The resulting electronic parameters are reported in the text.

molecules in this particular structure. That packing is sensitive to chain length is also seen in the small variations of exciton splitting with aggregate size described elsewhere in this section.

Relative Oscillator Strengths of the Exciton Bands. Experimentally, we find that, as the length of the DNA chain is increased, the oscillator strength of the lowermost exciton state gradually decreases with respect to the uppermost exciton state (Figure 3c−e and Table 1). This is due to the fact that the relative oscillator strengths of these two electronic transitions are sensitive to the relative orientation of the transition dipole moments of the dimers within a given aggregate.[13,26,53,54] These differences may therefore reflect small distortions in the double-helical structure of the short DNA segments as compared to that of the polymeric DNA that, in turn, affect the packing of the dimers within each aggregate.

Stark Spectra and Fit. The electronic properties of DiSC$_2$-(5) monomers are obtained from the analysis of the Stark spectra obtained at the magic angle ($\chi = 54.7$). Figure 6 shows the absorption (dotted) and electroabsorption (solid) spectra of DiSC$_2$(5) monomers when the spectra are obtained in the absence of DNA in 80% EG−water glass (Figure 6a) and when the DiSC$_2$(5) is bound to a duplex DNA in the monomeric form

Stark Spectroscopy of Helical H-Aggregates
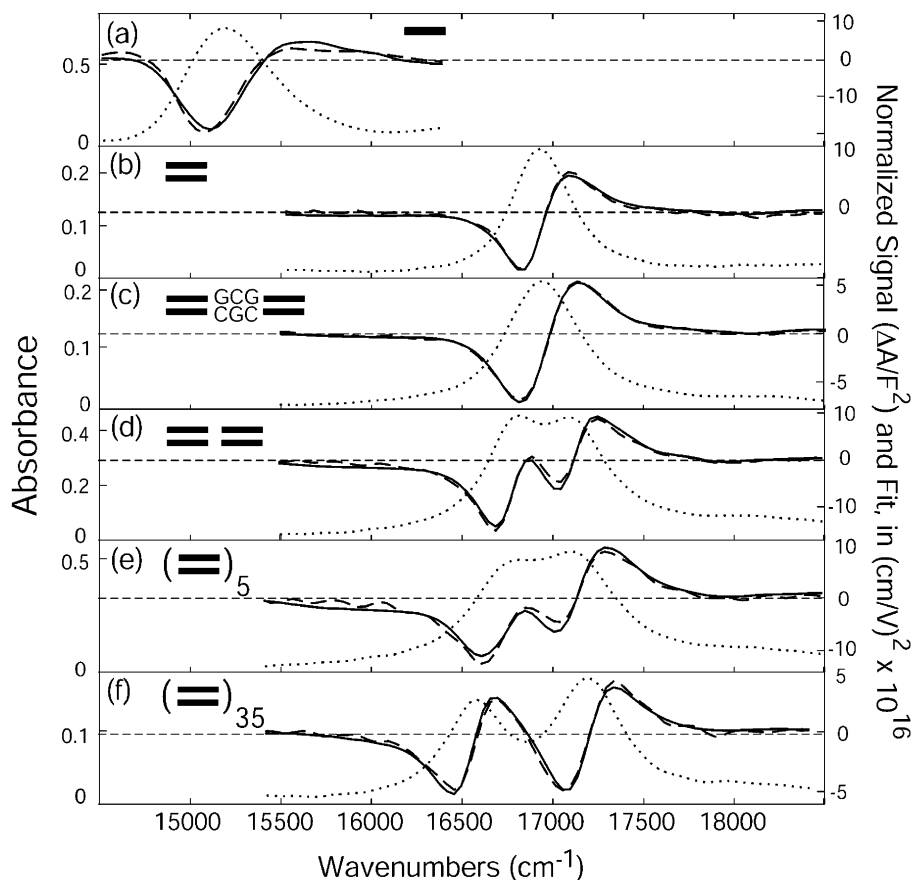
J. Phys. Chem. A, Vol. 107, No. 18, 2003 **3357**

Figure 7. 77 K absorption spectra (dotted), electroabsorption signal (solid) and the fit (dashed) to the electroabsorption signal at $\chi = 54.7°$ for (a) DiSC$_2$(5) monomer in the absence of duplex DNA duplex, (b) a single isolated H-dimer, (c) two H-dimers separated by three guanine−cytosine base pairs, (d) two adjacent H-dimers, (e) five adjacent H-dimers, and (f) ∼35 adjacent H-dimers. Each of the heavy bars in the legend represents a dye monomer.

TABLE 2: Electroabsorption Results for the Cyanine Monomer and H-Aggregates[e]

| | DiSC$_2$(5) monomer[a] | DNA templates used to form H−aggregates | | | |
		(IC)$_5$	(IC)$_{10}$	(IC)$_{25}$	poly(dI-dC)
no. of H-dimers	0.5	1	2	5	35 ± 5
abs max[b]	15 200	16 930	16 810	16800	16 580
			17 100	17100	17 200
$\langle \underline{\underline{\Delta\alpha}} \rangle$[c]	−16 (2)	−32 (4)	−30 (4)	−34 (4)	−36 (4)
$\|\underline{\Delta\mu}\|$[d]	1.1 (0.1)	0.9 (0.1)	0.7 (0.1)	0.55 (0.05)	0.45 (0.05)

[a] In the absence of DNA in a 77 K glass. [b] In cm^{-1}. [c] In Å^3. [d] In D. [e] Errors are shown in parentheses

(Figure 6b). Interestingly, the wavelength maxima and the line shape of the absorption and of the electroabsorption spectra of the monomer in these two environments are very similar. The absorbance of the dye monomers bound to DNA is very low (∼0.04), resulting in a noisy absorption and electroabsorption signal. The fit (dashed lines in Figure 6) to the Stark signal using the derivatives of the absorption spectra, for dye monomers bound to DNA yields values of the electronic properties ($\langle \underline{\underline{\Delta\alpha}} \rangle = -14 \pm 3$ Å^3 and $|\underline{\Delta\mu}| = 0.8 \pm 0.1$ D) that are similar to those obtained for the monomeric dyes in solution (glass) in the absence of DNA templates (see Table 2). These results demonstrate that *it is valid to compare the properties of the aggregates bound to DNA with those of the monomer in solvent glass as the DNA minor groove appears to only weakly perturb the absorption spectrum of this dye.*

Information regarding how the electronic properties of the helical H-aggregates scale both with the extent of exciton

coupling and the number of molecules comprising the aggregate is obtained from analysis of the Stark spectra shown in Figure 7. The solid lines in Figure 7 represent the electroabsorption spectra at the magic angle ($\chi = 54.7°$) and the dashed lines represent the fit to the Stark signal using the derivatives of the absorption spectrum. In presence of the DNA templates (Figure 7b−f) there is no significant absorption or electroabsorption signal in the monomer region of the spectrum (14 000−15 500 cm^{-1}), showing that the majority of the DiSC$_2$(5) molecules are bound to the DNA in the form of aggregates. Likewise, the electric field does not induce additional transitions beyond those seen in the field-free spectrum. Remarkably good fits to the electroabsorption signal were obtained for all of the H-aggregate systems (Figure 7b−f) throughout the full absorption range (15 500−18 500 cm^{-1}). This indicates a uniform field response of the electronic states involved in the transitions therefore suggesting that the DNA templates afford very homogeneous aggregate structures.

From the fit to the electroabsorption signal, the change in the average electronic polarizability ($\langle \underline{\underline{\Delta\alpha}} \rangle$) and the change in the dipole moment ($|\underline{\Delta\mu}|$) between the ground and the excited electronic states for the monomer and the H-aggregates were evaluated. The significance of the values of $\langle \underline{\underline{\Delta\alpha}} \rangle$ and $|\underline{\Delta\mu}|$ obtained from the fits (Table 2) are discussed below.

Experimental Values of $\langle \underline{\underline{\Delta\alpha}} \rangle$ of Monomer and Aggregates. The monomer of DiSC$_2$(5) was found to have a negative value of $\langle \underline{\underline{\Delta\alpha}} \rangle$ (−16 Å^3) as has also been seen previously for cationic cyanine dyes in polar environments.[52,55,56] For a single H-dimer ((IC)$_5$ sequence), the value of $\langle \underline{\underline{\Delta\alpha}} \rangle$ is −32 Å^3, which is twice that of the value of the monomeric dye
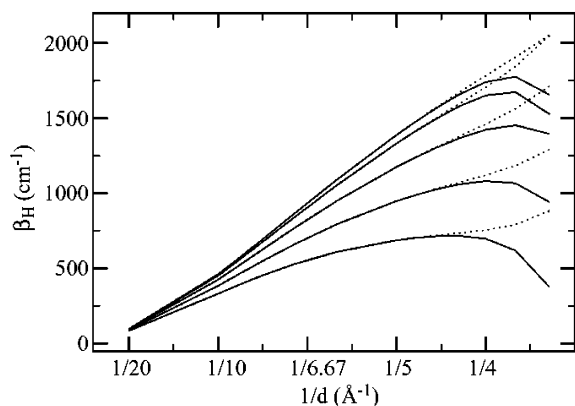
Figure 8. Coupling energy β_H resulting from H-dimer formation as a function of inverse spacing $1/d$, calculated from the shift of the dominant one-photon state from its location in the monomer. Five different shifts, $s = 0, 1, 2, 3,$ and 4 Å, are shown in order from top to bottom. The solid (dotted) lines show the results obtained with (without) inclusion of charge-transfer between monomers.
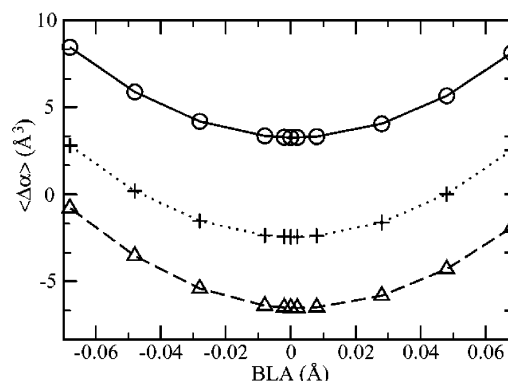

Figure 9. Average polarizability change, $\langle \Delta\alpha \rangle$, as a function of bond-length alternation (BLA) for a planar monomer ($\circ - \circ$), and monomers with a twist of 50° ($+ \cdot \cdot \cdot +$) and 100° ($\triangle$ - - $\triangle$) between the rings on either end of the dye (see Experimental Section).

in solution. Interestingly, for the $(IC)_{10}$ sequence, where two adjacent H-dimers interact in a head-to-tail fashion, the measured value of $\langle \Delta\alpha \rangle$ (-30 Å^3) does *not* further increase compared to that of the single isolated dimer. This indicates that head-to-tail coupling between neighboring H-dimers has little effect on the $\langle \Delta\alpha \rangle$ of the system and that the enhancement factor for $\langle \Delta\alpha \rangle$ is 2 for all aggregates studied.

To further examine the effect of the secondary coupling on the value of $\langle \Delta\alpha \rangle$, we investigated an aggregate system where two H-dimers are separated by three guanine−cytosine base pairs ($^2(IC)_5$ duplex DNA), such that the γ_H is minimal (i.e., splitting is unresolved in the absorption spectrum, Figure 7c, dotted line). The fit to the electroabsorption signal (Figure 7c, dashed line) for this system yields a value of $\langle \Delta\alpha \rangle$ that is identical ($\langle \Delta\alpha \rangle = -33$ Å^3) with that of the two adjacent H-dimers. Likewise $\langle \Delta\alpha \rangle$ remains constant (-34 to -36 Å^3) *even* for longer DNA templates ($(IC)_{25}$ and poly(dI−dC)) which have somewhat higher values of γ_H ($210-320$ cm^{-1}).

Similar results were obtained earlier for H-aggregates of another similar cyanine dye ($DiSC_{3+}(5)$) that can form both H- and J-aggregates in the presence of poly(dI−dC) DNA.[52] For these polymeric H-aggregates, the value of $\langle \Delta\alpha \rangle$ was also found to be equal to twice that of the monomer. In contrast, the value of $\langle \Delta\alpha \rangle$ for the polymeric J-aggregates was found to be $4-6$ times that of the monomer. The weaker scaling of $\langle \Delta\alpha \rangle$ with size in H-aggregates vs *J*-aggregates is possibly correlated to the smaller value of the exciton coupling ($165-320$ cm^{-1}) for the former as compared to the large splitting seen in the latter (~ 600 cm^{-1}).[52] In ref 52, it was argued that this coupling is larger for the J-aggregates because their brickwork structure affords better overlap between dyes adjacent to one another on the helical chain.

Calculated Effect of Aggregate Structure on β_H and γ_H. To determine whether the observed coupling β_H is consistent with the model summarized in Figure 4, we calculated β_H between planar cyanine dyes as a function of the face-to-face spacing, d, and the lateral shift, s, which are defined in the Experimental Section. The results are summarized as the solid lines in Figure 8. The turnover at short distances is due to charge transfer between dyes, as shown by the dotted lines which are the results obtained with charge-transfer suppressed. The experimental coupling $\beta_H \sim 1750$ cm^{-1} is reproduced with a value of d of about 4 Å and a value of s that is less than 1 Å. Though the DNA template is expected to induce a twist in the

dimer structure, our calculations indicate that this will alter β_H by only 4% (data not shown).[57]

We next consider the coupling between adjacent H-dimers, γ_H. For reasonable dimer parameters ($d = 3.9$ Å and $s = 0$) and with a distance between the H-dimers such that the closest approach between hydrogen atoms is 2.5 Å, the calculated coupling between the H-dimers is $\gamma_H = 550$ cm^{-1}. This is larger than the experimental value of ~ 200 cm^{-1}, which we attribute to dielectric screening between the transition moments of the two H-dimers that is not included in the calculations. Because of the close packing of dyes within a single H-dimer, screening is not expected to have a large effect on the calculated β_H.

The fact that the calculated β_H and γ_H are consistent with the experimental results supports the assignment of the electronic transitions of Figure 4 and suggests that our geometric model of the aggregates (Figure 2) is reasonable.

Calculations of $\langle \Delta\alpha \rangle$ for the Monomer and Aggregates. Experiments showed that the value of $\langle \Delta\alpha \rangle$ *doubled* from -16 to -32 Å^3 on formation of a dimer but did *not* further increase for higher aggregates. Here we discuss the results of our efforts to model this behavior computationally.

We begin by examining $\langle \Delta\alpha \rangle$ of the monomer. The transition from a polyene-like structure to a cyanine-like structure causes $\langle \Delta\alpha \rangle$ to go from a value that is large and positive to a value that is near zero or small and negative, in certain molecules.[55] Such changes can be induced experimentally by varying solvent polarity and can be modeled computationally by varying the BLA of the system.[55,56,58−60] In addition to BLA, $\langle \Delta\alpha \rangle$ is expected to be sensitive to twisting of the dye, as the resulting loss of conjugation should impact the polarizability of the excited state more strongly than that of the ground state.

Figure 9 shows the calculated $\langle \Delta\alpha \rangle$ as a function of the BLA for a planar dye and dyes with twist angles of 50° (crosses) and 100° (triangles) between rings (see Experimental Section). As expected, $\langle \Delta\alpha \rangle$ decreases with twist angle and has its minimum value in the cyanine limit of zero BLA. Although negative values of $\langle \Delta\alpha \rangle$ are obtained for small BLA and substantial twist angles, the magnitudes are smaller than those seen experimentally, particularly as the DNA template is expected to induce a twist of only $\sim 20°$.

In addition to the above structural effects, we also explored two environmental effects on $\langle \Delta\alpha \rangle$ of the monomer. Environmental disorder was modeled by surrounding the system with a lattice of randomly oriented dipoles.[61] We also included dielectric screening of electron−hole interactions in the excited states.[61] Inclusion of these environmental effects increases

Stark Spectroscopy of Helical H-Aggregates

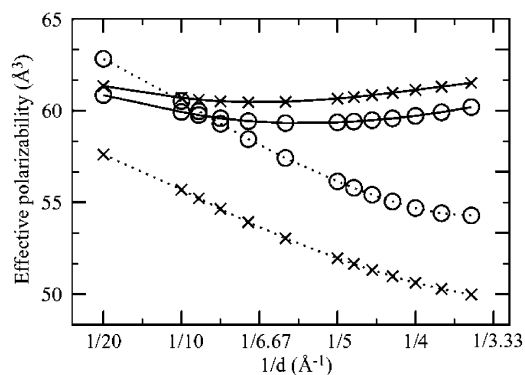*J. Phys. Chem. A, Vol. 107, No. 18, 2003* **3359**

Figure 10. Effective average polarizabilities of the ground state $\langle\alpha_{GS}^{dimer}\rangle/2$ (dotted lines) and the dominant one-photon excited state $\langle\alpha_{ES}^{dimer}\rangle - (\langle\alpha_{GS}^{dimer}\rangle/2)$ (solid lines) as a function of the inverse interplane spacing $1/d$. The crosses ($\times$) are for the planar structure of Figure 2a, and the circles ($\bigcirc$) are for monomers with a twist of 50° between the rings.

$\langle\underline{\Delta\alpha}\rangle$ of the monomer toward more positive values, and so again cannot account for the observed negative $\langle\underline{\Delta\alpha}\rangle$ for this species. A nearby counterion does, however, lower the calculated $\langle\underline{\Delta\alpha}\rangle$. For example, placing a fluoride ion in the plane of the dye molecule on the side of the two nitrogen atoms, centered and 3 Å away from the closest hydrogen in the polyene chain, changes the monomer's $\langle\underline{\Delta\alpha}\rangle$ by -8 Å³.

The above lack of numerical agreement between experiment and theory on the monomer can perhaps be attributed to slight inaccuracies in the quantum chemical treatment of the system (finite field INDO/SCI) especially as the observed $\langle\underline{\Delta\alpha}\rangle$ is at most 10% of the ground state polarizability. Despite this numerical disagreement, we would expect the calculations to be able to reproduce the experimentally observed trend in $\langle\underline{\Delta\alpha}\rangle$ with aggregate formation. However, we will see below that this is not the case.

We begin by considering a dimer in which coupling leads to coherence between the monomers but has a negligible effect on the state energies and transition moments. The fluorescence lifetime of such a dimer is predicted to be half that of the monomer and so the lifetime can be considered a direct measure of the coherence length, N_C. The polarizability of the ground state (GS) and excited state (ES) of such a dimer can be expressed in terms of the corresponding quantities of the monomer as shown in eq 5,

$$\alpha_{GS}^{dimer'} = 2\alpha_{GS}^{monomer}; \quad \alpha_{ES}^{dimer'} = \alpha_{GS}^{monomer} + \alpha_{ES}^{monomer} \tag{5}$$

where the prime indicates the assumption that coupling between monomers does not influence the state energies or transition moments (see Appendix). Unlike the fluorescence lifetime, the assumption of coherence alone is not sufficient to alter $\langle\underline{\Delta\alpha}\rangle$ of the dimer from that of the monomer. Instead, the effects of aggregation on $\langle\underline{\Delta\alpha}\rangle$ must arise from the effects of coupling between the monomers on the state energies and transition moments. These are investigated next.

To remove the trivial scaling of the polarizability with the number of noninteracting monomers (eq 5), we plot effective polarizabilities for the ground and excited state, $\langle\alpha_{GS}^{dimer}\rangle/2$ and $\langle\alpha_{ES}^{dimer}\rangle - (\langle\alpha_{GS}^{dimer}\rangle/2)$, in Figure 10. These quantities isolate the effects that shifts in the energies and transition moments have on the ground and excited-state polarizabilities. Results are shown for H-dimers formed from monomer structures having either positive or negative values of $\langle\underline{\Delta\alpha}\rangle$ (i.e. planar vs nonplanar). For both structures, the polarizability of the ground
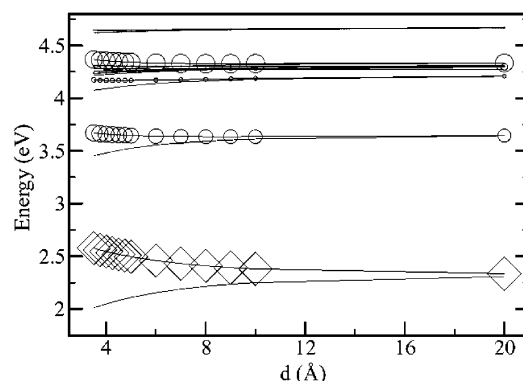

Figure 11. Energies of the excited states as a function of interplane separation, d, for H-dimers with no lateral shift, $s = 0$, and with a SCI basis that does not allow charge transfer between monomers. The size of the symbols corresponds to the magnitude of the transition moments, with diamonds for the transition between the ground state and one-photon excited state; and circles for the transition between the dominant one-photon state and the two-photon states.

state decreases, while that of the excited state increases. *The calculations therefore predict that* $\langle\underline{\Delta\alpha}\rangle$ *will become more positive on formation of dimer, independent of the initial sign of* $\langle\underline{\Delta\alpha}\rangle$. This is in contradiction to the experimental results where $\langle\underline{\Delta\alpha}\rangle$ becomes more *negative* on H-dimer formation.

The origin of the calculated changes in $\langle\underline{\Delta\alpha}\rangle$ was explored by examining the excited state energies and transition moments, which are shown in Figure 11 for an H-dimer consisting of two planar monomers. Since coupling has only small effects on the transition moments, we focus on the excited state energies. The decrease in the polarizability of the ground state (Figure 10) can be connected to the increase in the energy gap between the ground state and the state that carries most of the one-photon intensity. The opposite is seen for the optically excited state, where the gap between this state and the higher energy states decreases on formation of a dimer. Since the calculated change in $\langle\underline{\Delta\alpha}\rangle$ seems to be a direct consequence of the calculated splittings of Figure 11, the disagreement with the experimentally observed $\langle\underline{\Delta\alpha}\rangle$ may indicate that these calculated splittings are not reliable. It is also possible that the disagreement between experiment and theory indicates that $\langle\underline{\Delta\alpha}\rangle$ is influenced by double excitations in a manner that is not captured by finite-field SCI theory.[62]

Another potential origin of the disagreement between the observed and calculated $\langle\underline{\Delta\alpha}\rangle$ is the presence of charge transfer between monomers, which is suppressed in Figures 10 and 11, but can substantially enhance $\langle\underline{\Delta\alpha}\rangle$ of the aggregate relative to that of the monomer.[63,64] Figure 12 shows the calculated $\Delta\alpha$ along the x, y, and z axes as a function of interplane spacing, d, both with and without inclusion of charge transfer between dyes. The results indicate that the principal effect of charge transfer is to introduce a change in polarizability along the axis connecting the two dyes, $\Delta\alpha_{zz}$. Since this component is positive, it cannot account for the experimentally observed decrease in $\langle\underline{\Delta\alpha}\rangle$. The magnitude of $\Delta\alpha_{zz}$ does, however, provide an experimental handle on the degree of charge transfer present in the excited state. Experimentally, $\Delta\alpha_{zz}$ is less than 25 Å³ (assuming $\Delta\alpha_{yy}$ to be zero, data not shown), which limits the charge transfer to less than 5%.

Although the predicted effects of dimer formation on $\langle\underline{\Delta\alpha}\rangle$ are not in agreement with experiment, agreement is found with regards to the effects of higher aggregation. The experimental results of Table 2 indicate that, while $\langle\underline{\Delta\alpha}\rangle$ changes substantially between the monomer and H-dimer, the coupling between
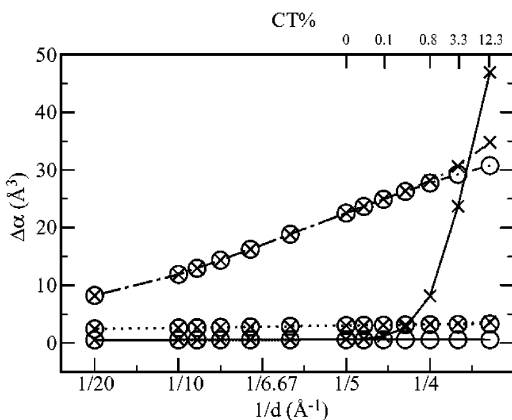
Figure 12. Change in polarizability between excited and ground electronic states, $\underline{\underline{\Delta\alpha}}$, as a function of interplane separation, *d*. The dotted-dashed line $(\overline{\overline{= \cdot -}})$ shows $\Delta\alpha_{xx}$, the dotted line (•••) shows $\Delta\alpha_{yy}$, and the solid line shows $\Delta\alpha_{zz}$. The monomers are parallel to the *xy* plane and displaced from one another along the *z*-axis.. The crosses (circles) show the results obtained with (without) inclusion of charge transfer between monomers. The top axis shows the percent charge transfer in the excited state. The principle effect of charge transfer is an increase in the polarizability along the axis connecting the monomers, $\Delta\alpha_{zz}$.

H-dimers has little effect on $\langle\underline{\underline{\Delta\alpha}}\rangle$. Calculations are in agreement with this trend, as the $\overline{\overline{\text{predicted}}}$ $\langle\underline{\underline{\Delta\alpha}}\rangle$ for two adjacent dimers is the same as that for a single $\overline{\text{dimer}}$ to within 10%.

Change in the Dipole Moment ($|\underline{\Delta\mu}|$). Both in a solvent glass and when bound to the DNA minor groove, monomeric DiSC$_2$(5) has a small value of $|\underline{\Delta\mu}|$, indicating that the excited electronic states have little charge-transfer character. This is not surprising for a symmetric cyanine in which a dipole must arise from symmetry breaking either due to nonzero BLA or disorder. Comparably small values of $|\underline{\Delta\mu}|$ have been reported by Grewer et al. for symmetric cyanines of similar structure.[65]

The values of $|\underline{\Delta\mu}|$ for the different H-aggregates (0.45−0.9 D) are found to be slightly smaller than that for the monomeric DiSC$_2$(5) (1.1 D). That $|\underline{\Delta\mu}|$ for the H-aggregates is smaller than the value for the monomeric dye is in agreement with the theoretical predictions by Dubinin,[66] who showed that the $|\underline{\Delta\mu}|$ for the aggregate is less than or equal to the value for the constituent monomers. In the special case of dimers, the $|\underline{\Delta\mu}|$ for the monomer and the dimer can be directly related using eq 6, derived in ref 66:

$$\cos 2\theta = \left[\frac{|\vec{\Delta}\mu_{\text{dimer}}|}{|\vec{\Delta}\mu_{\text{monomer}}|} \right] \quad (6)$$

where θ is the angle between the transition moments of the individual monomers. Equation 6 predicts that the maximum value of the $|\underline{\Delta\mu}|$ for an aggregate is that of the monomer if all the constituent dyes in the aggregate are parallel to each other. Since the transition moments of the monomers within the dimer should be roughly parallel, we expect $|\underline{\Delta\mu}|$ of the dimer to be roughly equal to that of the monomer as is found to be the case (Table 2). Because of the structure of the helical template, we expect θ to be ~90° between adjacent H-dimers.[26] We then expect coupling between adjacent H dimers to lower $|\underline{\Delta\mu}|$, as is seen experimentally.

It is noteworthy that the value of $|\underline{\Delta\mu}|$ of DiSC$_2$(5) monomers bound to the DNA minor groove (~0.8 D) is slightly smaller than that of the monomers in 80% EG−water glass in the absence of DNA (1.1 D). It is possible that the dipoles of the adjacent monomers on the DNA strand experience a weak head-to-tail interaction with one another, resulting in a reduction of the value of the $|\underline{\Delta\mu}|$ relative to the value in the solvent glass.

Summary and Conclusions

The primary goal of this work was to assess whether the enhancement factor for $\langle\underline{\underline{\Delta\alpha}}\rangle$ provides an alternative method of characterizing N_C for aggregates, as was suggested in ref 38. For both H- and J-type aggregates, independent measures of N_C have been obtained here and in ref 52, respectively. Due to the different photophysical properties of these two types of aggregates, the source of the independent measure is necessarily different. We have previously seen that, for J-aggregates, the value of N_C obtained from line width and fluorescence lifetime measurements agrees with the enhancement factor for $\langle\underline{\underline{\Delta\alpha}}\rangle$ to within a factor of 2.[52] For H-aggregates, the saturation $\overline{\overline{\text{of}}}$ the spectral splitting due to interaction between H-dimers ($2\gamma_{\text{H}}$) can be taken as a direct measure of N_C. This saturation occurs at an aggregate size of greater than six adjacent H dimers, implying $N_C > 12$. This value for N_C differs considerably from the enhancement factor for $\langle\underline{\underline{\Delta\alpha}}\rangle$ of 2 observed for these systems.

The different relations between the enhancement factor for $\langle\underline{\underline{\Delta\alpha}}\rangle$ and N_C for J- and H-aggregates may be rationalized on a geometric basis. In J-aggregates, the brickwork geometry leads to strong coupling of each dye with two neighbors, while the geometry of the H-aggregate leads to strong coupling within a dimer and much weaker coupling between adjacent dimers. This is reflected in the ratio of *intra*dimer ($\boldsymbol{\beta}$) to *inter*dimer ($\boldsymbol{\gamma}$) coupling strengths, which is 2:1 in J-aggregates[52] and 10:1 in H-aggregates. Because the intradimer and interdimer interactions are quite similar in J-aggregates, the enhancement of $\langle\underline{\underline{\Delta\alpha}}\rangle$ can be expected to be sensitive to both types of coupling $\overline{\overline{\text{and}}}$ so dependent on the overall coherence, N_C. In H-aggregates, $\langle\underline{\underline{\Delta\alpha}}\rangle$ is dominated by intradimer couplings as evidenced by $\overline{\overline{\text{its}}}$ enhancement factor saturating at a single H-dimer. Since the enhancement factor of $\langle\underline{\underline{\Delta\alpha}}\rangle$ depends only on the intradimer coupling, it is not surprising that it is equal to 2, which is the number of strongly coupled monomers, rather than the overall coherence length, N_C, which is established by the much weaker interdimer coupling.

The results presented here and elsewhere[52] indicate that the enhancement factor of $\langle\underline{\underline{\Delta\alpha}}\rangle$ is related to the number of *strongly* coupled dyes in the aggregate. The observation of this scaling behavior is particularly interesting, as an explanation in terms of simple models or quantum chemical calculations remains elusive.

Appendix

This section considers the polarizability of a dimer in which coupling leads to coherence between the monomers but has a negligible effect on the state energies and transition moments. The fluorescence lifetime of such a dimer is predicted to be half that of the monomer, and so the lifetime can be considered a direct measure of the coherence length. Here, we show that

Stark Spectroscopy of Helical H-Aggregates

J. Phys. Chem. A, Vol. 107, No. 18, 2003 **3361**

$\Delta\alpha$ of such a dimer is the same as that of the monomer, and so this property does not have a direct dependence on coherence length that is analogous to that of the fluorescence lifetime.

The polarizability of the ground state (GS) and excited state (ES) of such a dimer can be expressed in terms of the corresponding quantities of the monomer by beginning with the sum over states expression for the polarizability

$$\alpha_i = \sum_{j \neq i} \frac{|\langle j|\hat{\mu}|i\rangle|^2}{E_j - E_i} \tag{A1}$$

where E_i is the energy of state $|i\rangle$, $\hat{\mu}$ is the dipole operator, and α_i is the polarizability of state $|i\rangle$. For convenience, we consider only a single tensor component of α_i such that $\hat{\mu}$ of eq A1 can be viewed as the x component of the dipole operator with α_i being the xx component of the polarizability.

The following notation is introduced for the properties of the monomer. The transition moments of the monomer are defined as

$$\langle b|\mu|a\rangle = \mu_{b,a} \tag{A2}$$

that the polarizabilities of the ground state and the ath excited electronic state are

$$\alpha_{GS}^{\text{monomer}} = \sum_{a \neq 0} \frac{|\mu_{a,0}|^2}{E_a} \tag{A3}$$

and

$$\alpha_{ES}^{\text{monomer}} = -\frac{|\mu_{a,0}|^2}{E_a} + \sum_{\substack{b \neq a \\ b \neq 0}} \frac{|\mu_{b,a}|^2}{E_b - E_a} \tag{A4}$$

where the index 0 refers to the ground state.

The relevant, parity-adapted, states of the dimer are

$$|GS^+\rangle = |0,0\rangle \tag{A5}$$

$$|a^\pm\rangle = \frac{1}{\sqrt{2}}[|a,0\rangle \pm |0,a\rangle] \tag{A6}$$

$$|(a,b)^\pm\rangle = \frac{1}{\sqrt{2}}[|a,b\rangle \pm |b,a\rangle]; \ a \neq b \tag{A7}$$

$$|(a,a)^+\rangle = |a,a\rangle \tag{A8}$$

where $|a,b\rangle$ denotes a state of the dimer in which the first monomer is in state a and the second monomer is in state b, and the superscripts indicate parity. Equation A5 is the ground state of the dimer, eq A6 represents the states in which only one monomer is excited and eqs A7 and A8 are the states in which both monomers are excited. The relevant transition moments of the dimer can be expressed in terms of those of the monomer as

$$\langle GS|\mu|a^+\rangle = \sqrt{2}\mu_{0,a} \tag{A9}$$

$$\langle a^\pm|\mu|b^\pm\rangle = \mu_{a,b} \tag{A10}$$

$$\langle (a,b)^\pm|\mu|a^\pm\rangle = \mu_{0,b} \tag{A11}$$

$$\langle (a,a)^+|\mu|a^+\rangle = \sqrt{2}\mu_{0,a} \tag{A12}$$

The polarizability of ground state of the dimer may then be written as

$$\alpha_{GS}^{\text{dimer}} = \sum_{a \neq 0} \frac{|\langle a^+|\mu|GS\rangle|^2}{E_a} = 2\sum_{a \neq 0} \frac{|\mu_{a,0}|^2}{E_a} = 2\alpha_{GS}^{\text{monomer}}$$

The polarizability of the optically allowed $|a^+\rangle$ excited state may then be written as

$$\alpha_{ES}^{\text{dimer}} = -\frac{|\langle GS|\mu|a^+\rangle|^2}{E_a} + \sum_{b \neq a} \frac{|\langle b^+|\mu|a^+\rangle|^2}{E_b - E_a} +$$

$$\sum_{b \neq a} \frac{|\langle (a,b)^+|\mu|a^+\rangle|^2}{E_b} + \frac{|\langle (a,a)^+|\mu|a^+\rangle|^2}{E_a} =$$

$$-2\frac{|\mu_{a,0}|^2}{E_a} + \sum_{\substack{b \neq a}} \frac{|\mu_{b,a}|^2}{E_b - E_a} + \sum_{\substack{b \neq a \\ b \neq 0}} \frac{|\mu_{b,0}|^2}{E_b} + 2\frac{|\mu_{a,0}|^2}{E_a} =$$

$$\alpha_{GS}^{\text{monomer}} + \alpha_{ES}^{\text{monomer}} \tag{A13}$$

Thus, $\Delta\alpha^{\text{dimer}} = \Delta\alpha^{\text{monomer}}$, and the assumption of coherence alone is not sufficient to alter the change in polarizability.

References and Notes

(1) Special Issue on Light Harvesting Physics Workshop. *J. Phys. Chem. B* **1997**, *101*, 7197−7359.

(2) Mukamel, S.; Chemla, D. S., Eds. Special Issue on Confined Excitations in Molecular and Semiconductor Nanostructures. *Chem. Phys.* **1996**, *210*.

(3) Gilman, P. B. J. *Photog. Sci. Eng.* **1974**, *18*, 418−430.

(4) Kawagishi, H.; Morikawa, Y.; Kurihara, S.; Kasanuki, J. Liquid Crystal Display with Fluorescent Light Source Illumination. Patent Jpn. Kokai Tokkyo Koho Japan, 1992.

(5) Wang, Y. *Chem. Phys. Lett.* **1986**, *126*, 209−214.

(6) Deisenhopfer, J.; Epp, O.; Mikki, K.; Huber, R.; Michel, H. *J. Mol. Biol.* **1984**, *180*, 385−398.

(7) Jelly, E. E. *Nature (London)* **1936**, *138*, 1009−1010.

(8) Scheibe, G. *Angew. Chem.* **1936**, *49*, 563.

(9) Brooker, L. G. S.; White, F. L.; Heseltine, D. W.; Keyes, G. H.; Dent, S. G.; Van Lare, E. J. *J. Photogr. Sci.* **1953**, *1*, 173−183.

(10) Herz, A. H. *Photogr. Sci. Eng.* **1974**, *18*, 323−335.

(11) McRae, E. G.; M. K. *J. Chem. Phys.* **1958**, *28*, 721−722.

(12) Kasha, M. *Radiat. Res.* **1963**, *20*, 55−70.

(13) McRae, E. G.; Kasha, M. The Molecular Exciton Model. *Physical Processes in Radiation Biology*; Academic Press: New York, 1964; pp 23−42.

(14) Kasha, M.; Rawls, H. R.; El-Bayoumi, M. A. *Pure Appl. Chem.* **1965**, *11*, 371−392.

(15) Kasha, M. *Molecular Excitons in Small Aggregates*; Plenium Press: New York, 1976.

(16) Davydov, A. S. *Theory of Molecular Excitons*; McGraw-Hill: New York, **1962.**

(17) Norland, A. K.; Ames, A.; Taylor, T. *Photogr. Sci. Eng.* **1970**, *14*, 295−307.

(18) Bohn, P. W. *Annu. Rev. Phys. Chem.* **1993**, *44*, 37−60.

(19) Harrison, W. J.; Mateer, D. L.; Tiddy, G. J. T. *J. Phys. Chem.* **1996**, *100*, 2310−2321.

(20) De Rossi, U.; Daehne, S.; Lindrum, M. *Langmuir* **1996**, *12*, 1159−1165.

(21) Khairutdinov, R. F.; Serpone, N. *J. Phys. Chem. B* **1997**, *101*, 2602−2610.

(22) Moll, J.; Harrison, W. J.; Brumbaugh, D. V.; Muenter, A. A. *J. Phys. Chem. A* **2000**, *104*, 8847−8854.

(23) Scheblykin, I. G.; Bataiev, M. M.; Van der Auweraer, M.; Vitukhnovsky, A. G. *Chem. Phys. Lett.* **2000**, *316*, 37−44.

(24) Seifert, J. L.; Connor, R. E.; Kushon, S. A.; Wang, M.; Armitage, B. A. *J. Am. Chem. Soc.* **1999**, *121*, 2987−2995.

(25) Wang, M.; Silva, G. L.; Armitage, B. A. *J. Am. Chem. Soc.* **2000**, *122*, 9977−9986.

(26) Yaron, D.; Armitage, B. A.; Raheem, I.; Kushon, S.; Seifert, J. L. *Nonlinear Opt.* **2000**, *26*, 257−264.

(27) Fidder, H.; Knoester, J.; Wiersma, D. A. *Chem. Phys. Lett.* **1990**, *171*, 529−536.

(28) De Boer, S.; Wiersma, D. A. *Chem. Phys. Lett.* **1990**, *165*, 45−53.

(29) McIntire, M. J.; Manas, E. S.; Spano, F. C. *J. Chem. Phys.* **1997**, *107*, 8152−8164.

(30) Potma, E. O.; Wiersma, D. A. *J. Chem. Phys.* **1998**, *108*, 4894−4903.

(31) Spano, F. C.; Kuklinksi, J. R.; Mukamel, S. *J. Chem. Phys.* **1991**, *94*, 7534−7544.

(32) Knapp, E. W. *Chem. Phys.* **1984**, *85*, 73−82.

(33) Bakalis, L. D.; Knoester, J. *J. Lumin.* **2000**, *87−89*, 66−70.

(34) Mobius, D.; Kuhn, H. *Isr. J. Chem.* **1979**, *18*, 375−384.

(35) Feller, K. H.; Gadonas, R.; Krasauskas, V.; Fidler, V.; Vajda, S. *Laser Chem.* **1991**, *11*, 1−12.

(36) Misawa, K.; Kobayashi, T. *Nonlinear Opt.* **1996**, *15*, 81−84.

(37) De Boer, S.; Vink, K. J.; Wiersma, D. A. *Chem. Phys. Lett.* **1987**, *137*, 99−106.

(38) Misawa, K.; Kobayashi, T. *Nonlinear Opt.* **1995**, *14*, 103−120.

(39) Kobayashi, T. *Mol. Cryst. Liq. Cryst.* **1998**, *314*, 1−11.

(40) Murakami, H.; Morita, R.; Watanabe, T.; Asai, K.; Honma, I.; Zhou, H.; Yamashita, M.; Ishigure, K.; Shigekawa, H. *Mol. Cryst. Liq. Cryst.* **1999**, *327*, 31−35.

(41) Wendt, H.; Friedrich, J. *Chem. Phys.* **1996**, *210*, 101−107.

(42) In the original work by Armitage and co-workers, adenine-thyamine base pairs were used in the templating regions for the smaller DNA sequences. However, at 77 K, stronger binding of the dye to the DNA was observed using the inosine−cytosine sequences.

(43) Locknar, S. A.; Peteanu, L. A. *J. Phys. Chem. B* **1997**, *102*, 4240−4246.

(44) Premvardhan, L. L.; Peteanu, L. A. *J. Phys. Chem. A* **1999**, *103*, 7506−7514.

(45) Chowdhury, A.; Locknar, S. A.; Premvardhan, L. L.; Peteanu, L. A. *J. Phys. Chem. A* **1999**, *103*, 9614−9625.

(46) Liptay, W. Dipole Moments and Polarizabilities of Molecules in Excited Electronic States. In *Excited States*; Lim, E. C., Ed.; Academic Press: New York, 1974; Vol. 1; pp 129−229.

(47) Bublitz, G. U.; Boxer, S. G. *Annu. Rev. Phys. Chem.* **1997**, *48*, 213−242.

(48) Frisch, J.; Trucks, G. W.; Schlegel, H. B.; Scuseria, G. E.; Robb, M. A.; Cheeseman, J. R.; Zakrzewski, V. G.; J. A. Montgomery, J.; Stratmann, R. E.; Burant, J. C.; Dapprich, S.; Millam, J. M.; Daniels, A. D.; Kudin, K. N.; Strain, M. C.; Farkas, O.; Tomasi, J.; Barone, V.; Cossi, M.; Cammi, R.; Mennucci, B.; Pomelli, C.; Adamo, C.; Clifford, S.; Ochterski, J.; Petersso, G. A.; Ayala, P. Y.; Cui, Q.; Morokuma, K.; Malick, D. K.; Rabuck, A. D.; Raghavachari, K.; Foresman, J. B.; Cioslowski, J.; Ortiz, J. V.; Stefanov, B. B.; Liu, G.; Liashenko, A.; Piskorz, P.; Komaromi, I.; Gomperts, R.; Martin, R. L.; Fox, D. J.; Keith, T.; Al-Laham, M. A.; Peng, C. Y.; Nanayakkara, A.; Gonzalez, C.; Challacombe, M.; Gill, P. M. W.; Johnson, B.; Chen, W.; Wong, M. W.; Andres, J. L.; Gonzalez, C.; Head-Gordon, M.; Replogle, E. S.; Pople, J. A. Gaussian 98, Revision A.6. Gaussian, Inc.: Pittsburgh, PA, 1998.

(49) Kurtz, H. A.; Stewart, J. J. P.; Dieter, K. M. *J. Comput. Chem.* **1990**, *11*, 82−87.

(50) Tomlinson, A.; Yaron, D. J. *J. Comput. Chem.*, submitted for publication.

(51) Pasquinelli, M. An Effective Particle Approach to the Photophysics of Conjugated Polymers. Ph.D. Thesis, Carnegie Mellon University, 2002.

(52) Chowdhury, A.; Wachmann-Hogiu, S.; Bangal, P. R.; Raheem, I.; Peteanu, L. A. *J. Phys. Chem. B* **2001**, *105*, 12196−12201.

(53) Gallos, L. K.; Pimenov, A. V.; Scheblykin, I. G.; Van der Auweraer, M.; Hungerford, G.; Varnavsky, O. P.; Vitukhnovsky, A. G.; Argyrakis, P. *J. Phys. Chem. B* **2000**, *104*, 3918−3923.

(54) Spitz, C.; Knoester, J.; Ourat, A.; Daehne, S. *Chem. Phys.* **2002**, *275*, 271−284.

(55) Bublitz, G. U.; Ortiz, R.; Marder, S. R.; Boxer, S. G. *J. Am. Chem. Soc.* **1997**, *119*, 3365−3376.

(56) Bublitz, G. U.; Ortiz, R.; Runser, C.; Fort, A.; Barzoukas, M.; Marder, S. R.; Boxer, S. G. *J. Am. Chem. Soc.* **1997**, *119*, 2311−2312.

(57) The calculated β_H of Figure 8 is based on the shift in energy of the one-photon allowed state between monomer and dimer, since this is how β_H is derived from experiment. These values for β_H differ somewhat from those obtained by taking the splitting between the bright and dark electronic states resulting from H-aggregate formation, since the center of these two states shifts relative to the monomer by about 400 cm^{-1} for $d = 4$ Å.

(58) Marder, S. R.; Gorman, C. B.; Meyers, F.; Perry, J. W.; Bourhill, G.; Breédas, J.-L.; Pierce, B. M. *Science* **1994**, *265*, 632−635.

(59) Meyers, F.; Marder, S. R.; Pierce, B. M.; Brédas, J. L. *J. Am. Chem. Soc.* **1994**, *116*, 10703−10714.

(60) Locknar, S. A.; Peteanu, L. A.; Shuai, Z. *J. Phys. Chem. A* **1999**, *103*, 2197−2201.

(61) Wachsmann-Hogiu, S.; Peteanu, L. A.; Liu, L. A.; Yaron, D. J.; Wildeman, J. *J. Phys. Chem. B*, submitted for publication.

(62) For the ground electronic state, finite field Hartree−Fock theory is equivalent to the Random Phase Approximation (RPA), which is in turn, similar to a sum-over-states calculation at the SCI level (Parkinson, W. A.; Zerner, M. C. *Chem. Phys. Lett.* **1987**, *139*, 563−570). This suggests that finite-field methods are analogous to a sum-over-states approach that includes all excited states that would arise from single excitations out of the state to which the field is applied. Therefore by analogy, we expect the excited polarizability from finite field SCI (FF/SCI) theory to include effects from all states that would arise from single excitations out of the SCI excited state, i.e. states that include double excitations. FF/SCI theory is used here instead of doubles CI because FF/SCI is size-consistent and we are comparing $\langle \Delta\alpha \rangle$ between systems of very different size.

(63) Somsen, O. J. G.; Chernyak, V.; Frese, R. N.; van Grondelle, R.; Mukamel, S. *J. Phys. Chem. B* **1998**, *102*, 8893−8908.

(64) Middendorf, T. R.; Mazzola, L. T.; Lao, K.; Steffen, M. A.; Boxer, S. G. *Biochim. Biophys. Acta* **1993**, *1143*, 223−234.

(65) Grewer, G.; Losche, M. Electrooptical Investigation of Two-Dimensional Aggregated Chromophore Systems. *Dynamical Processes in Condensed Molecular Systems*; Proceedings of the Emiurg Symposium, Thurnau, Germany, 1990.

(66) Dubinin, N. V. *Opt. Spectrosc. (USSR)* **1977**, *43*, 49−51.